PHYSICAL REVIEW B **76**, 201306(R) (2007)

Enhancement of electron and hole effective masses in back-gated GaAs/$Al_xGa_{1-x}As$ quantum wells

S. Nomura,[1,2,3,*] M. Yamaguchi,[2,3] T. Akazaki,[2,3] H. Tamura,[2,3] T. Maruyama,[4] S. Miyashita,[4] and Y. Hirayama[5,6]
[1]*Institute of Physics, University of Tsukuba, Tennodai, Tsukuba 305-8571, Japan*
[2]*NTT Basic Research Laboratories, NTT Corporation, 3-1 Morinosato-Wakamiya, Atsugi 243-0198, Japan*
[3]*CREST-JST, 5 Sanbancho, Chiyoda, Tokyo 102-0075, Japan*
[4]*NTT Advanced Technology, 3-1 Morinosato-Wakamiya, Atsugi 243-0198, Japan*
[5]*Department of Physics, Faculty of Science, Tohoku University, 6-3 Aoba, Aobaku, Sendai 980-8578, Japan*
[6]*SORST-JST, 5 Sanbancho, Chiyoda, Tokyo 102-0075, Japan*
(Received 4 September 2007; revised manuscript received 19 October 2007; published 16 November 2007)

Both the electron and the optically created hole effective masses are found to be density dependent in a two-dimensional electron system of a GaAs/$Al_{0.33}Ga_{0.67}As$ back-gated quantum well by magnetophotoluminescence spectroscopy. We show that the density-dependent electron effective mass increases with a decrease in the electron density (n_s) to $n_s < 1 \times 10^{11}$ cm^{-2}. It is found that the electron effective masses determined from the lowest and the second Landau levels are larger than those from the higher Landau levels. The hole effective mass is found to increase with a decrease in n_s and the hole is found to localize at $n_s < 3 \times 10^{10}$ cm^{-2}. We observe an upward convex curve of the photoluminescence peak energy at $2 < \nu < 3$ depending on the electron-hole distance divided by the magnetic length. These results clearly show the important roles of both electron-electron and electron-hole interactions in the recombination of a valence hole with a high-quality two-dimensional electron system.

DOI: 10.1103/PhysRevB.76.201306 PACS number(s): 73.43.−f, 71.18.+y, 78.55.Cr, 78.20.Ls

Two-dimensional electron systems (2DESs) in the low-electron-density regime are excellent systems to investigate many-body phenomena induced by electron-electron interaction. With a decrease in the electron density (n_s), transition of the electron ground state to a ferromagnetic fluid phase was predicted before transition to the Wigner crystal phase.[1] Currently, it is still a challenge to detect these transitions experimentally in GaAs heterostructures, although there have been continuous efforts to realize a high-quality 2DES at low n_s by utilizing gated undoped structures.[2,3] Precursors to the transitions, such as the enhancement of the Landé g factor[4] and the electron effective mass (EEM), have been observed.[5] A back-gated undoped quantum well (QW) structure has advantages in investigating the properties of 2DESs in the low-n_s regime, because of the high tunability of n_s and the low degradation of the electron mobility at low n_s.[3] One of the advantages of using optical spectroscopy to investigate the properties of 2DESs in the low-n_s regime lies in the fact that the properties of both the insulating and the conducting phases of the 2DES are detected seamlessly. In the insulating phase, the peaks due to the neutral and the charged excitons dominate the photoluminescence (PL) spectra.[6] In the conducting phase, the PL reflects the properties of the 2DES, as evidenced by the observation of discontinuities of the optical transition energies and the peak intensities correlated with the integer and fractional filling factors ν.[7–13] Optical spectroscopy has been applied to measure the EEM and the hole effective mass (HEM) in semiconductors such as by interband magnetooptics[7,14,15] and by cyclotron resonance.[16–19] In the regime where the electron-electron interaction is weak, the effective masses obtained by both the methods should be identical. However, in the regime where the electron-electron interaction plays a large role, the renormalized effective mass deviates from the single-particle effective mass. The renormalized effective mass depends on parameters, such as n_s, ν, the index of the Landau level occupied by the electron, and the distance between the electron and the optically created hole. While a transport measurement probes the EEM at the Fermi energy, PL probes the effective masses of the electrons between the ground state and the Fermi energy. The PL measurements thus have an advantage in investigating the renormalized effective mass, which depends on the electron state, for example, the index of the Landau level at a fixed ν. There have been few systematic observations of the renormalized effective mass by magneto-PL. In this paper, we report results of systematic measurements of the EEM (m_e^*) and the HEM (m_h^*) as functions of n_s using the Shubnikov–de Haas (SdH) oscillation and magneto-PL.

The samples were single 50 nm GaAs QWs with the thickness of the $Al_{0.33}Ga_{0.67}As$ barrier layer varied from 250 and 400 nm. A thick n-type GaAs buffer layer was used as a rear contact. The samples have peak mobility of 3×10^6 cm^2/V s. The back-gate bias voltage was applied between the annealed contacts and the conducting n-GaAs layer. The conductance σ_{xx} of a Corbino device was measured between 0.4 and 1 K, in perpendicular magnetic fields. The laser light at 800 nm was introduced into a dilution refrigerator by an optical fiber with a 400 μm core diameter at the incident power of 1 μW. The unpolarized PL of $0.5 \times 0.5 - 1 \times 1$ mm^2 square mesa structures were measured at about 100 mK with a 1 m focal length monochromator. The effective masses are determined by the PL typically below 1 T. In this regime, the characteristic electron-electron interaction energy defined by $E_0 = \sqrt{\pi/2}e^2/(\epsilon\ell)$ is larger than the cyclotron energy $\hbar\omega_c$, where ℓ and ϵ are the magnetic length and the dielectric constant, and E_0 and $\hbar\omega_c$ are 5.6 and 1.7 meV, respectively, at 1 T.

Before proceeding to the discussion of the optical proper-

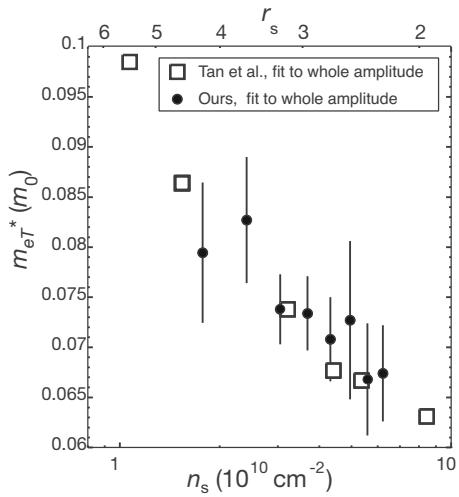

FIG. 1. Electron density dependence of the electron effective mass m_{eT}^* obtained by Shubnikov–de Haas measurements. The values in the literature (Ref. 5) are also shown.

ties of our samples, we show the results of the density-dependent EEMs obtained by a transport measurement. The EEM is determined from the temperature dependence of the amplitude of the oscillating part of the magnetoresistance.[5] The oscillating part of the magnetoresistance, $R_{xx} \propto 1/\sigma_{xx}$, is obtained by fitting the SdH curve to a sinusoidal curve in the low-magnetic-field regime, avoiding the quantum Hall regime. The EEMs are obtained from a $\ln(\Delta R_{xx}/T)$ vs T plot. Figure 1 shows that the obtained transport mass (m_{eT}^*) increases with a decrease in n_s. The agreement of the obtained values with those in the literature[5] indicates that the increase of m_{eT}^* with decrease in n_s is universal, irrespective of the structure or the peak mobility of the samples. This shows that the increase in m_{eT}^* is due to the electron-electron interaction, ruling out the role of disorder.

An alternative method for obtaining the electron-density-dependent EEM and HEM is to apply magneto-PL measurements. Here, we investigate the PL spectra of 2DESs in the regime where the pseudospin symmetry is violated. The electron-hole separation is made relatively large by using samples with QW width of 50 nm. In addition, we investigate in the regime where the mixing of the Landau levels is strong due to weak magnetic fields. Under these conditions, the PL spectra are expected to reflect the effect of the electron-electron interaction.

Figures 2(a)–2(d) show typical PL spectra and Landau-fan diagrams at $n_s=3.0\times10^{10}$ and 9.4×10^{10} cm^{-2}. The PL peaks due to the Landau levels are observed with the full width at half maximum of about 0.4 meV. The enhancement of the peak height of the peak at 1.5148 eV at $n_s=9.4\times10^{10}$ cm^{-2} is due to the Fermi-edge singularity.[20] The anomalies in PL at integer ν, seen in Figs. 2(c) and 2(d), also appeared in previous work.[8–12] Figure 3(a) shows the n_s dependence of the PL peak intensity in the vicinity of $\nu=1$. An anomalous decrease in the PL intensity is observed at $\nu=1$ for a wide range of n_s. It is possible to trace the anomaly at $\nu=1$ down to $n_s=8.6\times10^9$ cm^{-2} corresponding to $r_s=6$. This enables us to precisely determine n_s. The anomaly at $\nu=4/3$ is also observed, indicating the high quality of the sample.

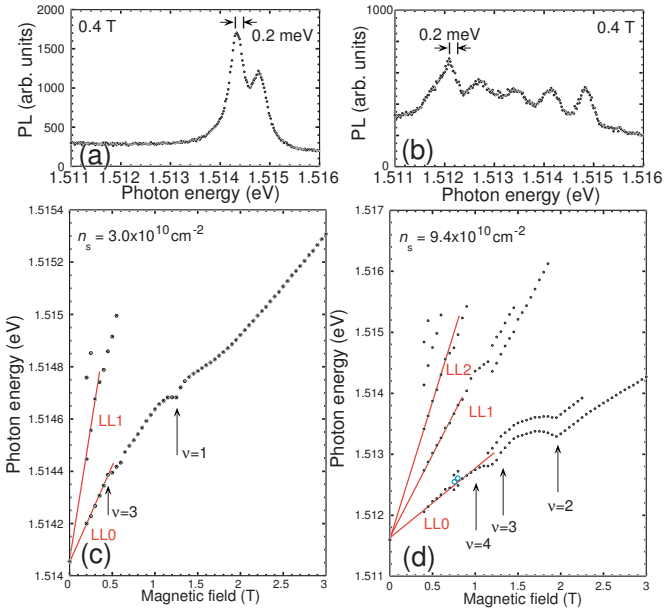

FIG. 2. (Color online) Typical PL spectra at n_s=(a) 3.0×10^{10} and (b) 9.4×10^{10} cm^{-2} at $B=0.4$ T. Landau-fan diagrams at n_s=(c) 3.0×10^{10} and (d) 9.4×10^{10} cm^{-2}. The best fitted lines are shown (solid lines). Data points indicating the average of the transition energies of the Zeeman split peaks are also shown (circles); they are included in the linear fitting procedure.

The PL peaks between $\nu=2$ and 3 show deviation from the linear dependence on B and show an upward convex curve as depicted in Fig. 3(b). This behavior is explained by a calculation by Asano and Ando.[12] Although their calculation was performed for the high-magnetic-field limit of $E_0 \ll \hbar\omega_c$, which does not hold in our experiment, the calculation qualitatively explains the upward convex curve. The observed upward shift from the reference energy is about

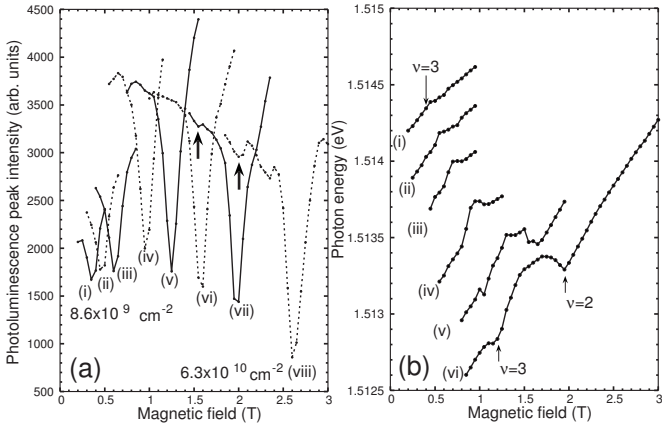

FIG. 3. (a) Electron density dependence of the PL peak intensity in the vicinity of $\nu=1$ at n_s=0.86 (i), 1.2 (ii), 1.6 (iii), 2.3 (iv), 3.0 (v), 3.9 (vi), 5.1 (vii), and 6.3×10^{10} cm^{-2} (viii). An anomaly is observed at $\nu=1$ in the PL peak intensity. An anomaly at $\nu=4/3$ (arrows) is also observed at (vii) and (viii). (b) Electron density dependence of the PL peak position between $\nu=2$ and 3, at n_s=3.0 (i), 3.9 (ii), 5.1 (iii), 6.3 (iv), 7.5 (v), and 9.4×10^{10} cm^{-2} (vi), showing the upward convex curve.

$0.05E_0$, which is smaller than the calculated upward shift of about $0.2E_0$. This smaller shift in our experiment is consistent with the fact that the mixing of the higher Landau levels (LLs) by the Coulomb interaction weakens the interaction effect. It should be noted that the bowing effect is only present in LL0, and the LL1 peak shows linear dependence on B. The PL peak energy depending on B shows only a small feature at $\nu=3$ for low n_s. By assuming a constant e-h distance d, d/ℓ decreases with a decrease in B. For the limiting case of $d/\ell=0$, a kind of pseudospin symmetry survives, and thus the interaction energies are constant.

In the regions of $\nu>3$ and $1<\nu<2$, the PL peak energies ($E_{\mathrm{LL}Ne}$) are fitted by

$$\frac{dE_{\mathrm{LL}Ne}}{dB}=\frac{e\hbar}{m_0}\left[\frac{1}{m^*_{e,\eta}}\left(N_e+\frac{1}{2}\right)+\frac{1}{m^*_h}\left(N_h+\frac{1}{2}\right)\right], \qquad (1)$$

where $m^*_{e,\eta}$ and m^*_h are the EEM and the HEM, respectively, N_e and N_h are the Landau indices for the electron and the hole, respectively, m_0 is the electron mass in the vacuum, and η is the index. The peak energies are obtained by spectral fittings to symmetric and asymmetric Lorentzian curves for the LLN ($N\geq 1$) and LL0 peaks, respectively, at $B\neq 0$ T. The band-edge energy at 0 T is obtained by spectral fittings to a function for a 2D joint density of states with a broadening parameter.[21]

In the low-n_s regime, the EEMs depend on the index of the Landau levels because of the electron-electron and electron-hole interactions. The PL peaks due to the transition between N_e and $N_h=0$ are observed at low temperatures. The off-diagonal ($N_e\neq N_h$) transitions are induced by the mixing of the Landau-levels and by the impurity scattering. The slopes of three peaks, $dE_{\mathrm{LL}0}/dB$, $dE_{\mathrm{LL}1}/dB$, and $dE_{\mathrm{LL}2}/dB$, are obtained by fitting on the Landau-fan diagrams in magnetic fields typically below 1 T. Four unknown variables, the EEMs for LL0, LL1, and LL2, and the HEM, cannot be determined by three equations. Then, the EEMs, m^*_{e10} and m^*_{e21} are derived by $m^*_{e10}=(e\hbar/m_0)(dE_{\mathrm{LL}1}/dB-dE_{\mathrm{LL}0}/dB)^{-1}$ and $m^*_{e21}=(e\hbar/m_0)(dE_{\mathrm{LL}2}/dB-dE_{\mathrm{LL}1}/dB)^{-1}$. These masses are regarded as the "average" masses of the electrons in the two adjacent Landau levels. They coincide with the cyclotron mass in the limiting case of the weak interaction. At filling factors such as $\nu=2$, 3, and 5, double peaks are observed due to the spin splitting. We used the average of the transition energies of the Zeeman splitted peaks for the linear fitting procedure in the case where the spin splitting is resolved. This is because we are considering the case where the energy shift is described by a spin-independent single-particle picture as in Eq. (1), and the other contributions are taken into account by a renormalized mass. The HEM is derived by $m^*_{h10}=(e\hbar/m_0)(3dE_{\mathrm{LL}0}/dB-dE_{\mathrm{LL}1}/dB)^{-1}$, and $m^*_{h21}=(e\hbar/m_0)(5dE_{\mathrm{LL}1}/dB-3dE_{\mathrm{LL}2}/dB)^{-1}$. These values should be identical in principle. However, because the estimated errors are markedly larger in m^*_{h21} than m^*_{h10}, we set $m^*_h=m^*_{h10}$, which is plotted in Fig. 4(b). The obtained hole energy per tesla, $e\hbar/2m^*_h m_0$, is found to be smaller than the estimated errors in $dE_{\mathrm{LL}0}/dB$ or $dE_{\mathrm{LL}1}/dB$ at $n_s<3.0\times10^{10}$ cm^{-2}. In this case, we set $m^*_h=\infty$ and regard the hole as localized.

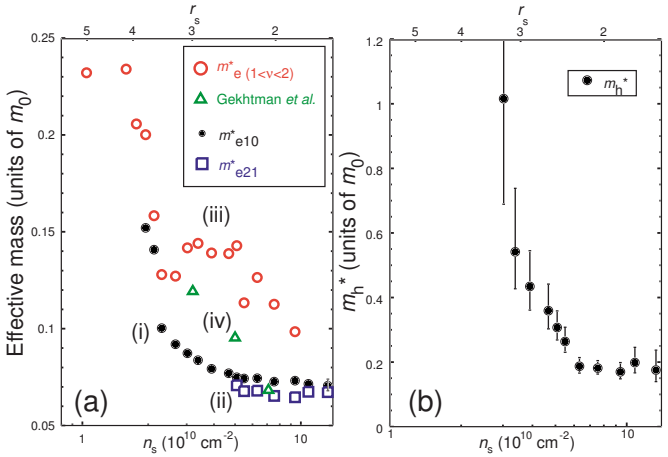

FIG. 4. (Color online) (a) Electron density dependence of the electron effective masses m^*_{e10} (i), m^*_{e21} (ii), and $m^*_{e(1<\nu<2)}$ (iii), derived from fitting to the Landau-fan diagrams. The values in the literature (Ref. 15) are also shown (iv). (b) Electron density dependence of the hole effective mass m^*_h.

The obtained effective masses m^*_{e10}, m^*_{e21}, and m^*_h increase with a decrease in n_s as shown in Fig. 4. The estimated errors in m^*_{e10} and m^*_{e21} are $\pm0.001-\pm0.003$. We have checked by a micro-PL measurement that the spatial density inhomogeneities, which can be a possible source of error, are small. The characteristic electron-electron interaction energy $E_0=\sqrt{\pi/2}e^2/(\epsilon\ell)$ is larger than the Fermi energy (ϵ_F), where E_0 is 5.6 meV at 1 T, and $\epsilon_F<3.6$ meV at $n_s<1\times10^{10}$ cm^{-2}. Then all the electron states contributing to the PL are mixed by the Coulomb interaction. The EEMs are n_s dependent, for the contributions not only from the electrons near the Fermi level, but also from the electrons in the lowest Landau level.

It is found that the EEMs derived from LL0 and LL1, m^*_{e10}, are systematically larger than those derived from LL2 and LL1, m^*_{e21}. At $n_s=1.3\times10^{11}$ cm^{-2}, $m^*_{e10}=0.070m_0$, which is 5% larger than $m^*_{e21}=0.067m_0$. It is also found that m^*_{e21} agrees with the SdH effective mass m^*_{eT}. At $r_s\sim4$, an increase of the EEM about 25% above the band mass was reported by cyclotron resonance[18] and the SdH (Ref. 22) measurements for density-dependent EEMs in Si inversion layers, which appears to be consistent with m^*_{eT} in Fig. 1. The obtained m^*_{10} is about 50% above the GaAs band mass at $r_s\sim4$, which is markedly larger than m^*_{eT} and other reported values. These results indicate that the increase in the obtained effective masses depends on the strength of the interactions on the electrons in the Landau levels. Clearly, the electron-hole interaction is larger between the electrons in LL0 and a hole in LL0 than between the electrons in the higher Landau levels and a hole in LL0, which recombine by off-diagonal transitions. Note here that the PL measurements were performed at the weak optical excitation limit. The average distance between photocreated holes is estimated to be about 100 μm by assuming the absorption coefficient $\alpha=1\times10^4$ cm^{-1},[23] and the population decay rate $\tau=0.4$ ns.[24] Then, it is unlikely that any optical excitation-power dependence of the effective mass would be observed in a PL measurement without a significant increase of the electron temperature.

Gekhtman *et al.* obtained the EEM by tuning n_s by illuminating modulation-doped QW samples above the barrier band gap[15] as shown in Fig. 4(a). While the overall tendency of the increase of m_e^* agrees with our results, their estimated values are larger than our values. The source of the disagreement is not clear but may be attributed to the difference in the method of tuning n_s.

The HEM increases from $m_h^*=0.18m_0$ to $1.0m_0$ with a decrease in n_s. The HEMs determined by our measurement in the high-density regime agree with the previous estimation of $m_h^*=0.159m_0$.[14] Figure 4 shows that the hole localizes at $n_s<3.0\times10^{10}$ cm^{-2} due to inefficient screening of the potential disorder by the electrons. The impact of the electron-hole interaction on the HEM has not been investigated yet. In the limit of large n_s, the overlap of the many-body wave function Φ with a hole at $\mathbf{r}$ is orthogonal to Φ' with a hole at $\mathbf{r}'$ by the Anderson orthogonality theorem.[20] This argument predicts enhancement of the HEM with an increase in n_s, which is contrary to our experimental observation. The other explanation would be that the apparent enhancement of the HEM stems from the density- and magnetic-field-dependent disorder potential. However, a sudden drop of the EEM in Si inversion layers was observed with a decrease in n_s below a threshold density, accompanied by a decrease in the scattering time.[18] This suggests that it is not appropriate to ascribe the enhancement of the HEM only to the disorder potential, although the role of disorder in Si inversion layers for the observed effective mass may differ from that in a GaAs 2DES. There are currently few theories available to account for the effect of disorder in the electrons on a hole in the low-density regime.

The PL peak shift in the region $1<\nu<2$ follows linear dependence on B to a good approximation except for the anomaly at $\nu=1$. Since it is not possible to determine both m_e^* and m_h^* from a single E-B plot, values of m_e^* are derived by using m_h^* at $\nu>3$. At $n_s=9.4\times10^{10}$ cm^{-2}, $m^*_{e(1<\nu<2)}$ is $0.092m_0$, which is 1.4 times larger than m^*_{e21}. Although the increase in m^*_{e21} and m^*_{e10} with a decrease in n_s is not significant at $n_s>5\times10^{10}$ cm^{-2}, the increase in $m^*_{e(1<\nu<2)}$ is apparent in the whole region depicted in Fig. 4. This indicates larger roles of the electron-electron and electron-hole interactions at $\nu<2$, where the magnetic field restores the binding energy of the electrons-hole system.[6,9,15]

In conclusion, the electron density dependencies of the EEM and the HEM are investigated by the transport and the PL measurements. It is found that the EEMs derived from LL0 and LL1, m^*_{e10}, are systematically larger than those derived from LL2 and LL1, m^*_{e21}, and m^*_{e21} agrees with the SdH effective mass. It is also found that the HEM increases with a decrease in n_s and the hole localizes below a threshold density. While there is no theory to explain this observation, we speculate that it may be accounted for by a magnetic field and electron-density-dependent screening of the disorder potential.

We acknowledge fruitful discussions with T. Ogawa and K. Asano. This work was partly supported by a Grant-in-Aid for Scientific Research from the Japan Society for the Promotion of Science.

*snomura@sakura.cc.tsukuba.ac.jp

[1] C. Attaccalite, S. Moroni, P. Gori-Giorgi, and G. B. Bachelet, Phys. Rev. Lett. **88**, 256601 (2002).
[2] B. Kane, L. N. Pfeiffer, K. W. West, and C. K. Harnett, Appl. Phys. Lett. **63**, 2132 (1993).
[3] Y. Hirayama, K. Muraki, and T. Saku, Appl. Phys. Lett. **72**, 1745 (1998).
[4] E. Tutuc, S. Melinte, and M. Shayegan, Phys. Rev. Lett. **88**, 036805 (2002).
[5] Y.-W. Tan, J. Zhu, H. L. Stormer, L. N. Pfeiffer, K. W. Baldwin, and K. W. West, Phys. Rev. Lett. **94**, 016405 (2005).
[6] I. Bar-Joseph, Chem. Phys. **318**, 99 (2005).
[7] M. Skolnick, K. J. Nash, S. J. Bass, P. E. Simmonds, and M. J. Kane, Solid State Commun. **67**, 637 (1988).
[8] S. Katayama and T. Ando, Solid State Commun. **70**, 97 (1989).
[9] G. E. W. Bauer, Phys. Rev. B **45**, 9153 (1992).
[10] T. Tsuchiya, S. Katayama, and T. Ando, Surf. Sci. **361/362**, 376 (1996).
[11] P. Hawrylak and M. Potemski, Phys. Rev. B **56**, 12386 (1997).
[12] K. Asano and T. Ando, Phys. Rev. B **65**, 115330 (2002).
[13] S. Nomura, M. Yamaguchi, T. Akazaki, H. Tamura, H. Takayanagi, and Y. Hirayama, Physica E (Amsterdam) **34**, 292 (2006).
[14] W. Chen, M. Fritze, W. Walecki, A. V. Nurmikko, D. Ackley, J. M. Hong, and L. L. Chang, Phys. Rev. B **45**, 8464 (1992).
[15] D. Gekhtman, E. Cohen, A. Ron, and L. N. Pfeiffer, Phys. Rev. B **54**, 10320 (1996).
[16] K. Ensslin, D. Heitmann, H. Sigg, and K. Ploog, Phys. Rev. B **36**, 8177 (1987).
[17] E. Batke, H. L. Stormer, A. C. Gossard, and J. H. English, Phys. Rev. B **37**, 3093 (1988).
[18] T. A. Kennedy, R. J. Wagner, B. D. MacCombe, and D. C. Tsui, Solid State Commun. **21**, 459 (1977).
[19] C. M. Hu, E. Batke, K. Kohler, and P. Ganser, Phys. Rev. Lett. **75**, 918 (1995).
[20] G. D. Mahan, *Many-Particle Physics*, 3rd ed. (Plenum, New York, 2000).
[21] A. Pinczuk, J. Shah, H. L. Stormer, R. C. Miller, A. C. Gossard, and W. Wiegmann, Surf. Sci. **142**, 492 (1984).
[22] V. M. Pudalov, M. E. Gershenson, H. Kojima, N. Butch, E. M. Dizhur, G. Brunthaler, A. Prinz, and G. Bauer, Phys. Rev. Lett. **88**, 196404 (2002).
[23] M. Sturge, Phys. Rev. **127**, 768 (1962).
[24] S. Brown *et al.*, Surf. Sci. **305**, 42 (1994).